



Title	Formulation of energy loss due to magnetostriction to design ultraefficient soft magnets
Author(s)	Tsukahara, Hiroshi; Huang, Haodong; Suzuki, Kiyonori et al.
Citation	NPG Asia Materials. 2024, 16(1), p. 19
Version Type	VoR
URL	https://hdl.handle.net/11094/94926
rights	This article is licensed under a Creative Commons Attribution 4.0 International License.
Note	

The University of Osaka Institutional Knowledge Archive : OUKA

<https://ir.library.osaka-u.ac.jp/>

The University of Osaka

ARTICLE

Open Access

Formulation of energy loss due to magnetostriction to design ultraefficient soft magnets

Hiroshi Tsukahara^{1,2}, Haodong Huang³, Kiyonori Suzuki³ and Kanta Ono¹

Abstract

The mechanism of energy loss due to magnetostriction in soft magnetic materials was analytically formulated, and our experiments validated this formulation. The viscosity of magnetic materials causes the resistive force acting on magnetic domain walls through strain due to magnetostriction, and magnetic energy is eventually dissipated by friction even without eddy currents. This energy loss mechanism explains the frequency dependence of the excess loss observed in the experiments, and the excess loss is dominated by the contribution of magnetostriction when the magnetostriction constant exceeds approximately 20 ppm. The random anisotropy model was extended by considering the effect of local magnetostriction as a correction to the magnetocrystalline anisotropy. The effect of magnetostriction was considerably suppressed by the exchange-averaging effect. The estimated effective random magnetoelastic anisotropy for nanocrystalline α -Fe reached as low as 18.6 J/m³, but this static effect could not explain the high excess loss at high frequencies observed in the experiments. The results of this research could provide new design criteria for high-performance soft magnetic materials based on low magnetostriction to reduce the excess loss.

Introduction

Soft magnetic materials are one of the main components of electric motors that govern the energy efficiency of electric vehicles^{1–3}. Since reducing the core loss of soft magnetic materials is essential for improving the energy efficiency of motors, the core loss mechanism has been extensively studied. Conventionally, materials with high electrical resistance and low coercivity have focused on reducing the core loss. However, it has been reported that the core loss of amorphous and nanocrystalline materials is not always reduced by focusing on these two well-known aspects because of the considerable loss component commonly referred to as the excess loss^{4,5}. Thus, clarifying the origin of the core losses in advanced soft

magnetic materials and establishing new design criteria for efficient magnetic cores are indispensable.

Under the operation frequency of typical electric motors, the magnetization dynamics are governed almost entirely by the motions of magnetic domain walls. The coercivity reflects the extent to which the wall motions are hindered, and a low coercivity is needed to reduce the hysteresis loss. Nanocrystalline soft magnetic materials (NSMMs) are representative low coercivity materials due to the low random magnetocrystalline anisotropy of their nanostructure^{6–9}. Thus, the hysteresis loss of NSMMs is reduced, and the energy efficiency is greatly improved by nanoscale grain refinement. However, despite the low coercivity, eddy currents could still cause energy losses, i.e., classical and anomalous eddy current losses¹⁰.

Magnetization rotation causes eddy currents in magnetic materials, and eddy currents generate energy losses regardless of the coercivity. Since the strength of eddy currents depends on the temporal variation in magnetization, these energy losses depend on the frequency of the

Correspondence: Hiroshi Tsukahara (tsukahara@ap.eng.osaka-u.ac.jp) or Kiyonori Suzuki (Kiyonori.Suzuki@monash.edu) or Kanta Ono (ono@ap.eng.osaka-u.ac.jp)

¹Department of Applied Physics, Osaka University, Osaka 565-0871, Japan

²Institute of Multidisciplinary Research for Advanced Materials, Tohoku University, Sendai 980-8577, Japan

Full list of author information is available at the end of the article

external magnetic field. When the magnetization is uniformly rotated, the energy loss increases with the square of the operation frequency. This phenomenon is referred to as the classical eddy current loss^{11–13}. In addition to this classical effect, motions of the domain wall cause the anomalous eddy current loss, which typically increases with frequency to a power of 1.5^{14–16}. This additional loss is caused by the local eddy currents associated with the moving domain walls. The exponent of 1.5 is attributed to the changes in the number of active domain walls.

The energy losses due to eddy currents can be reduced by increasing the electrical resistance. Owing to their small thickness (typically $\sim 20 \mu\text{m}$), amorphous alloys and NSMMs exhibit high electrical resistance, and the classical eddy current loss is suppressed in these materials. In contrast, it has been reported that the excess loss in soft magnetic materials remains considerable even if the electrical resistance is high^{4,5}. This strongly suggests that the excess loss could be caused by a mechanism unrelated to eddy currents.

It has been reported, for both amorphous alloys¹⁷ and NSMMs¹⁸, that the excess loss depends on the saturation magnetostriction, although the mechanism underlying this correlation remains unknown. Recently, we conducted micromagnetic simulations, including an effective field due to magnetostriction, to clarify the energy loss mechanism in NSMMs¹⁹. Our simulation results showed that the strain due to the magnetic domain walls dissipated the magnetic energy induced by an external magnetic field. However, an analytical formulation is indispensable for identifying how magnetostriction generates energy loss in NSMMs.

In this paper, we formulated the mechanisms of coercivity and energy dissipation due to magnetostriction and validated the formulation via comparison with the experimental results. The former was accomplished by extending the random anisotropy model by including the effect of the local magnetoelastic anisotropy, while the latter was achieved by framing the energy loss due to the viscous resistance caused by magnetostriction based on the Landau–Lifshitz–Gilbert equation. The mean coercive field due to magnetostriction was reduced by the randomness of the crystal axis of the nanocrystallites within the exchange length, and uniaxial anisotropy could be caused in the presence of a domain wall. Nevertheless, we found these magnetoelastic effects to be too small to account for the mechanism of the high energy loss observed in the experiments. Thus, we must consider domain wall motions to explain the high energy loss observed in the experiments. When the domain wall in the magnetic material moves, the viscous resistance acts on the magnetic domain wall due to magnetostriction, and the viscosity of the magnetic material causes magnetic energy dissipation. We found that the energy loss

due to magnetostriction increased with the frequency of the external magnetic field to power of 1.5. This frequency dependence was the same as that of the excess loss observed in the experiments.

Models and methods

Extended random anisotropy model with the local magnetoelastic anisotropy

Electron spins interact with each other in the crystal lattice of a magnetic material^{20–27}. Since the interaction between electron spins is a function of the interatomic distance, lattice distortion affects the magnetic energy of the magnetic material. When strain ξ_{ij} occurs, the magnetic material contains magnetoelastic energy, which can be written as:

$$E_{\text{magel}} = (c_{12} - c_{11})(\xi_{11}e_{11} + \xi_{22}e_{22} + \xi_{33}e_{33}) - 4c_{44}(\xi_{12}e_{12} + \xi_{23}e_{23} + \xi_{31}e_{31}) \quad (1)$$

where c_{11} , c_{12} and c_{44} are elastic constants in cubic symmetry, and e_{ij} is the stress-free strain²⁸. The stress-free strain is a spontaneous distortion in a single crystal without external stress. The stress-free strain can be written as:

$$e_{ij} = \begin{cases} \frac{3}{2}\lambda_{100}(m_i^2 - \frac{1}{3}) & (i = j) \\ \frac{3}{2}\lambda_{111}m_i m_j & (i \neq j) \end{cases} \quad (2)$$

where λ_{100} and λ_{111} are magnetostriction constants and m_i is the normalized magnetization vector along the x_i direction. The stress-free strain can be obtained by the stabilization of the sum of the magnetoelastic energy E_{magel} and elastic energy E_{el} , which can be written as

$$E_{\text{el}} = \frac{1}{2}c_{11}(\xi_{11}^2 + \xi_{22}^2 + \xi_{33}^2) + 2c_{44}(\xi_{12}^2 + \xi_{23}^2 + \xi_{31}^2) + c_{12}(\xi_{22}\xi_{33} + \xi_{33}\xi_{11} + \xi_{11}\xi_{22}). \quad (3)$$

The magnetoelastic energy and elastic energy are functions of the magnetization and direction of the crystal axis. Since NSMMs comprise many nanocrystallites with random crystal axes^{29–32}, the stress-free strain is different between nanocrystallites even when the magnetization is uniformly oriented. A strain mismatch causes stress at the interface between the nanocrystallites, and the nanocrystallites interact mechanically. Hence, the strain inside the nanocrystallites deviates from the stress-free strain in NSMMs.

The strain can be decomposed into homogeneous strain $\bar{\xi}_{ij}$ and heterogeneous strain η_{ij} ^{33,34}. When the nanocrystallites are strained, a mean strain can occur in the NSMM. This strain is referred to as the homogeneous strain. An NSMM is an isotropic elastic and magnetostrictive material because of the random orientation of the crystal axis of the nanocrystallites. Figure 1 shows a

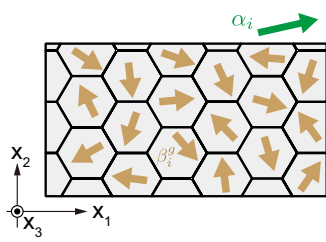


Fig. 1 Schematic illustration of the model for an NSMM. The system is constructed of nanocrystallites whose crystal axis is randomly oriented, and the strain distribution is nonuniform. α_i is the principal axis of the homogeneous strain. α_i points along the same direction for all of the nanocrystallites. β_i^g is the principal axis of the heterogeneous strain. The orientations of β_i^g randomly vary among the nanocrystallites.

schematic illustration of the model for the NSMM. In this paper, we assumed that the homogeneous strain can be written as:

$$\bar{\epsilon}_{ij} = \begin{cases} \lambda_w (\alpha_i^2 - \frac{1}{3}) & (i = j) \\ \lambda_w \alpha_i \alpha_j & (i \neq j) \end{cases} \quad (4)$$

where α_i is the principal axis of the homogeneous strain and λ_w denotes the strength of the homogeneous strain. Considering that the stress-free strain does not affect the nanocrystallite volume, we assumed that the homogeneous strain also does not affect the volume. Moreover, the strain exhibits a local structure, i.e., heterogeneous strain owing to the magnetic distributions and stresses between the nanocrystallites. We divided the magnetic material into nanocrystallite regions to analyze the effect of the heterogeneous strain. We assumed that the heterogeneous strain can be written as:

$$\eta_{ij}^g = \begin{cases} \lambda_d (\beta_i^g)^2 - \frac{1}{3} & (i = j) \\ \lambda_{od} \beta_i^g \beta_j^g & (i \neq j) \end{cases} \quad (5)$$

where g is an index for each nanocrystallite, β_i^g is a random unit vector, and λ_d and λ_{od} denote the strengths of the heterogeneous strains. The strain η_{ij}^g varies randomly between the nanocrystallites, and this strain also does not affect the volume of the nanocrystallites. Next, we can obtain the magnetoelastic energy using Eqs. (4) and (5). Substituting Eq. (4) into Eq. (1), we can obtain the magnetoelastic energy due to the homogeneous strain:

$$E_{\text{magel}}^h = K_u^h \sum_i^3 \left(\alpha_i^2 - \frac{1}{3} \right) \left(m_i^2 - \frac{1}{3} \right) + 2K_c^h \sum_{i \neq j}^3 \alpha_i \alpha_j m_i m_j. \quad (6)$$

In the above, the constants corresponding to the homogeneous strain can be defined as:

$$K_u^h = \frac{3}{2} (c_{12} - c_{11}) \lambda_{100} \lambda_w \quad (7)$$

$$K_c^h = -3c_{44} \lambda_{111} \lambda_w. \quad (8)$$

After rearranging Eq. (6), considering that α_i and m_i are unit vectors, we can obtain:

$$E_{\text{magel}}^h = (K_+^h + K_-^h) \left[(\alpha_1 m_1 + \alpha_2 m_2 + \alpha_3 m_3)^2 - \frac{1}{3} \right] - 4K_-^h (\alpha_1 \alpha_2 m_1 m_2 + \alpha_2 \alpha_3 m_2 m_3 + \alpha_3 \alpha_1 m_3 m_1), \quad (9)$$

where the effective anisotropic constants due to the homogeneous strain can be written as:

$$K_+^h = \frac{K_u^h + K_c^h}{2}, \quad K_-^h = \frac{K_u^h - K_c^h}{2}. \quad (10)$$

The first term of Eq. (9) corresponds to the uniaxial anisotropy. In the same way, we can obtain the magnetoelastic energy due to the heterogeneous strain, which can be written as:

$$E_{\text{magel}}^g = (K_+^G + K_-^G) \left[(\beta_1^g m_1 + \beta_2^g m_2 + \beta_3^g m_3)^2 - \frac{1}{3} \right] - 4K_-^G (\beta_1^g \beta_2^g m_1 m_2 + \beta_2^g \beta_3^g m_2 m_3 + \beta_3^g \beta_1^g m_3 m_1), \quad (11)$$

where the effective anisotropy constants due to heterogeneous strain are:

$$K_+^G = \frac{K_u^G + K_c^G}{2}, \quad K_-^G = \frac{K_u^G - K_c^G}{2}, \quad (12)$$

and the constants corresponding to the heterogeneous strain can be defined as:

$$K_u^G = \frac{3}{2} (c_{12} - c_{11}) \lambda_{100} \lambda_d \quad (13)$$

$$K_c^G = -3c_{44} \lambda_{111} \lambda_{od}. \quad (14)$$

The magnetizations within the exchange length are oriented along the same direction, and the magnetizations are collectively rotated by the external magnetic field. Hence, if there are many nanocrystallites within the exchange length, as in NSMMs, the magnetization dynamics are affected by the mean magnetoelastic energy. In the next step, we clarified the exchange softening effect of the magnetic anisotropy due to magnetostriction.

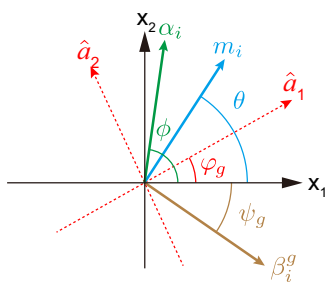


Fig. 2 Definition of the angles of the magnetization, crystal axes, α_i , and β_i^g . \hat{a}_1 and \hat{a}_2 denote the crystal axes. All quantities are rotated only in the x_1x_2 plane.

For simplicity of analysis, we assumed that the crystal axis, magnetization, α_i and β_i^g varied only in the x_1x_2 plane³⁵. Under this assumption, the magnetoelastic energy due to the homogeneous strain can be simply written as:

$$E_{\text{magel}}^h = (K_+^h + K_-^h) \left[(\alpha_1 m_1 + \alpha_2 m_2) - \frac{1}{3} \right] - 4K_-^h \alpha_1 \alpha_2 m_1 m_2. \quad (15)$$

The magnetization and principal axis of the homogeneous strain are oriented along the same direction between the nanocrystallites. In contrast, the unit vector β_i^g for the heterogeneous strain varies randomly. We defined the polar angles of those quantities as shown in Fig. 2, and Eq. (15) can be rewritten as:

$$E_{\text{magel}}^h = \frac{1}{2} K_+^h \cos 2(\theta - \phi) + \frac{1}{2} K_-^h \cos 2(\theta + \phi - 2\varphi_g) + \frac{1}{6} (K_+^h + K_-^h). \quad (16)$$

Note that Eqs. (4) and (5) are valid in a crystal frame in which the coordinate is established by the crystal axes. In the same way, the magnetoelastic energy due to the heterogeneous strain can be rewritten as:

$$E_{\text{magel}}^g = \frac{1}{2} K_+^G \cos 2(\theta - \psi_g) + \frac{1}{2} K_-^G \cos 2(\theta + \psi_g - 2\varphi_g) + \frac{1}{6} (K_+^G + K_-^G). \quad (17)$$

After shifting the origin of the magnetoelastic energy to remove constant terms, we can obtain:

$$E_{\text{magel}} = \frac{1}{2} K_+^h \cos 2(\theta - \phi) + \frac{1}{2} K_-^h \cos 2(\theta + \phi - 2\varphi_g) + \frac{1}{2} K_+^G \cos 2(\theta - \psi_g) + \frac{1}{2} K_-^G \cos 2(\theta + \psi_g - 2\varphi_g). \quad (18)$$

Nanocrystallites can also have magnetocrystalline anisotropy K_1 , which is usually greater than the anisotropy due to magnetostriction. When we consider cubic symmetry,

the magnetic anisotropy energy E_{ani} can be written as:

$$E_{\text{ani}} = -\frac{K_{\text{cry}}}{2} \cos 4(\theta - \varphi_g), \quad (19)$$

where $K_{\text{cry}} = K_1/4$. Hence, the total magnetic anisotropy energy E_{total} can be written as:

$$E_{\text{total}} = E_{\text{ani}} + E_{\text{magel}}. \quad (20)$$

Since magnetization is affected by the contributions of the nanocrystallites within the exchange length, we must consider a summation of the magnetoelastic energy. To obtain the amplitude of the summation of the total energy with respect to θ , we calculated the root mean square $\langle E_{\text{total}} \rangle$, which can be defined as:

$$\langle E_{\text{total}} \rangle = \frac{1}{N} \sqrt{\frac{1}{2\pi} \int_0^{2\pi} \left(\sum_{g=1}^N E_{\text{total}} \right)^2 d\theta}, \quad (21)$$

where N is the number of nanocrystallites within the exchange length. Note that we defined the root mean square of each nanocrystallite in Eq. (21). After a straightforward calculation and considering that ψ_g and φ_g are independently varied, we can obtain:

$$\langle E_{\text{total}} \rangle = \frac{1}{2\sqrt{2}} \sqrt{K_+^h{}^2 + \frac{1}{N} \left(K_-^h{}^2 + K_+^G{}^2 + K_-^G{}^2 + K_{\text{cry}}^2 \right)}. \quad (22)$$

After summation of the nanocrystallites, the magnetoelastic energy exhibits the lowest symmetry of anisotropy, i.e., uniaxial anisotropy, which can be written as:

$$E_{\text{total}} = \frac{1}{2} \langle K \rangle [1 - \cos 2(\theta - \varphi_K)], \quad (23)$$

where $\langle K \rangle$ is the random magnetic anisotropy, which includes a magnetostriction contribution, and φ_K denotes the direction of the uniaxial anisotropy. Since the root mean square of the oscillation term of Eq. (23) is $\langle K \rangle / 2\sqrt{2}$, the random magnetic anisotropy including magnetostriction contribution can be written as:

$$\langle K \rangle = \sqrt{K_+^h{}^2 + \frac{1}{N} \left(K_-^h{}^2 + K_+^G{}^2 + K_-^G{}^2 + K_{\text{cry}}^2 \right)}. \quad (24)$$

Next, we determined the dependence of the magnetic anisotropy constant due to magnetostriction on the nanocrystallite size. The number of nanocrystallites depends on the exchange length, which depends on the random magnetic anisotropy:

$$N = \frac{L_{\text{ex}}^3}{D^3}, \quad (25)$$

$$L_{\text{ex}} = \zeta \sqrt{\frac{A}{\langle K \rangle}}, \quad (26)$$

where L_{ex} is the exchange length, D is the diameter of the nanocrystallite, ζ is a constant corresponding to the symmetry of the magnetic anisotropy, and A is the exchange constant. Substituting Eqs. (25) and (26) into Eq. (24), we can obtain:

$$\langle K \rangle = \sqrt{K_+^h + \frac{\langle K \rangle^{\frac{3}{2}} D^3}{\zeta^3 A^{\frac{3}{2}}} (K_-^h + K_+^G + K_-^G + K_{\text{cry}}^2)}. \quad (27)$$

If K_+^h is negligible, the effective magnetic anisotropy is proportional to D^6 , i.e., we can obtain:

$$\langle K \rangle \simeq D^6 \left[\frac{1}{\zeta^3 A^{\frac{3}{2}}} (K_-^h + K_+^G + K_-^G + K_{\text{cry}}^2) \right]^2. \quad (28)$$

In contrast, when K_+^h is much larger than the other terms in Eq. (27), we can obtain:

$$\langle K \rangle \simeq K_+^h + \frac{D^3}{2\zeta^3 A^{\frac{3}{2}}} (K_-^h + K_+^G + K_-^G + K_{\text{cry}}^2) \sqrt{K_+^h}. \quad (29)$$

Figure 3 shows the nanocrystallite size dependency of the effective magnetic anisotropy $\langle K \rangle$ calculated by Eq. (27). The magnetic anisotropy due to magnetostriction exhibits the same trend as the random magnetocrystalline anisotropy when an induced anisotropy $K_u = K_+^h$ exists in the NSMM³⁶. When the mean magnetostriction is -8.9×10^{-6} , i.e., the NSMM comprises α -Fe nanocrystallites^{19,20}, the curve of $\langle K \rangle$ starts to deviate from Eq. (28). The induced anisotropy generated by the homogeneous strain is 18.6 J/m^3 , which is much smaller than the crystal anisotropy of α -Fe. With decreasing homogeneous strain, the effect of magnetostriction on the induced anisotropy also decreases. When λ_w is -0.89×10^{-6} , $\langle K \rangle$ is not sensitive to magnetostriction until the diameter of the nanocrystallite is smaller than 10 nm.

The homogeneous strain affects the motion of the magnetic domain wall in the same way as the induced anisotropy K_u , as expressed in Eq. (29). However, the effect of magnetostriction on the magnetic anisotropy energy depends on the mode of magnetization dynamics. When the magnetization is uniformly rotated in a magnetic material, the homogeneous strain also rotates, and the magnetoelastic energy is not affected by the homogeneous strain since the angle between m_i and α_i is constant. In this case, the homogeneous strain does not affect the effective magnetic anisotropy.

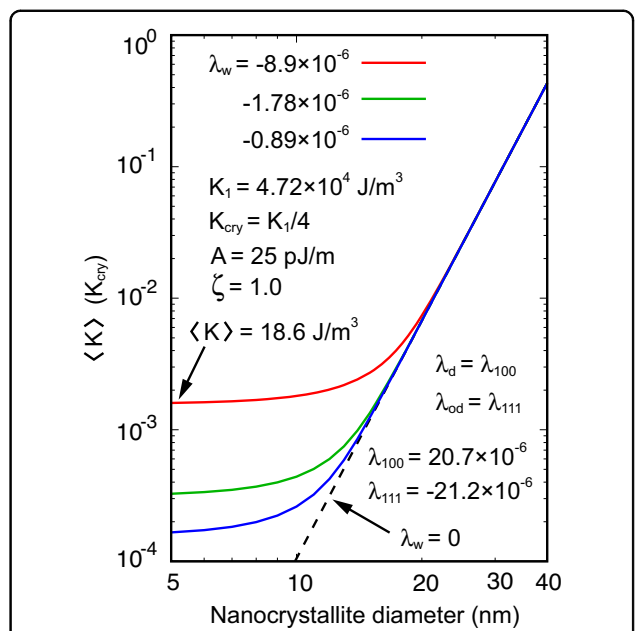


Fig. 3 Effective magnetic anisotropy $\langle K \rangle$, as calculated by Eq. (27). The red line is the effective magnetic anisotropy when λ_w is -8.9×10^{-6} , which is the homogeneous strain of the NSMM constructed by α -Fe nanocrystallites. The green and blue lines denote the effective magnetic anisotropy when λ_w is -1.78×10^{-6} and -0.89×10^{-6} , respectively. The elastic constants c_{11} , c_{12} , and c_{44} are 2.41×10^{11} , 1.46×10^{11} , and 1.12×10^{11} , respectively. λ_d and λ_{od} are the same as $\lambda_{100} = 20.7 \times 10^{-6}$ and $\lambda_{111} = -21.2 \times 10^{-6}$, respectively. The crystal anisotropy K_1 is $4.72 \times 10^4 \text{ J/m}^3$, the exchange stiffness constant A is 25 pJ/m , and ζ is 1.0.

However, the most important point conveyed by Fig. 3 is that the random magnetic anisotropy, including the magnetostriction contribution $\langle K \rangle$, cannot explain the excess loss, which is enhanced by the magnetostriction constant. Even if we consider the NSMM to be constructed of α -Fe nanocrystallites, the contribution to $\langle K \rangle$ is very small and independent of the frequency of the external magnetic field. Hence, we must consider other mechanisms of energy dissipation to explain the excess losses observed in the experiments⁵. In the following section, we formulate the mechanism of energy dissipation due to magnetostriction, focusing on changes in the strain caused by magnetic domain wall motion.

Energy dissipation due to magnetostriction by magnetic domain wall motion

Numerous magnetic domains are formed inside soft magnetic materials^{37–40}. When an external magnetic field is applied, the magnetic domain wall moves, and the strain distribution changes accordingly. Schematic illustrations of the strain distribution accompanying the magnetic domain wall are shown in Fig. 4. When static

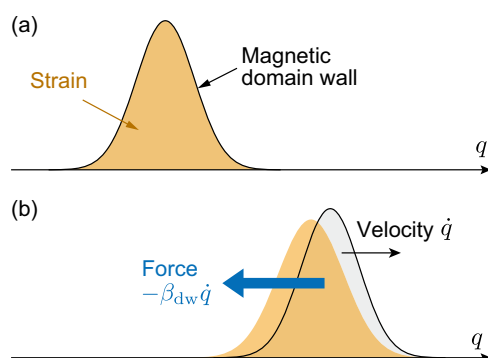


Fig. 4 Schematic illustrations of the strain distribution and magnetic domain wall. a Stability distribution of the strain caused by the magnetic domain wall. **b** Change in the strain distribution when the magnetic domain wall moves with velocity \dot{q} . The gray and orange colors indicate the magnetic domain wall region and the strain distribution, respectively.

magnetic domain walls produce stable strain distributions, the total energy, including the elastic energy, attains a local minimum value. Suppose that the magnetic domain wall moves due to the external magnetic field. In this case, the strain distribution also changes, but the change in the strain distribution is delayed because of the viscosity of the magnetic materials. Since this retardation causes an increase in the total energy, the viscous resistance acts on the magnetic domain wall to decrease the total energy. In the following, we formulate the energy loss due to the viscous resistance caused by magnetostriction based on the Landau–Lifshitz–Gilbert equation. When the strain changes with time, the elastic energy is dissipated due to internal friction. This energy dissipation is expressed by the dissipation function R , which can be written as:

$$R = \frac{1}{2}\zeta_{11}\left(\dot{\xi}_{11}^2 + \dot{\xi}_{22}^2 + \dot{\xi}_{33}^2\right) + 2\zeta_{44}\left(\dot{\xi}_{12}^2 + \dot{\xi}_{23}^2 + \dot{\xi}_{31}^2\right) + \zeta_{12}\left(\dot{\xi}_{22}\dot{\xi}_{33} + \dot{\xi}_{33}\dot{\xi}_{11} + \dot{\xi}_{11}\dot{\xi}_{22}\right), \quad (30)$$

where ζ_{ij} is the viscosity constant⁴¹. The strain can be obtained by calculating spatial derivatives of the displacement vector u_i , and the equation of motion can be expressed as:

$$\rho\ddot{u}_i - \frac{\partial}{\partial x_j}\left(\sigma_{ij} + \sigma'_{ij}\right) = 0, \quad (31)$$

where ρ is the mass density of the magnetic material, σ_{ij} is the stress caused by the strain ξ_{ij} , and σ'_{ij} is the dissipative stress due to the viscosity of solids. Hereinafter, repeated

subscripts are summed from 1 to 3. The stress and dissipative stress can be calculated as:

$$\sigma_{ij} = \frac{\partial E_{me}}{\partial \xi_{ij}}, \quad \sigma'_{ij} = \frac{\partial R}{\partial \dot{\xi}_{ij}}, \quad (32)$$

where E_{me} is the total energy caused by magnetostriction, which can be obtained as:

$$E_{me} = E_{magel} + E_{el}. \quad (33)$$

H. Suhl examined the contribution of magnetostriction to the magnetic damping constant by considering only the shear strains⁴². Following his theory, we can obtain the damping constant for magnetic domain wall motion due to magnetostriction. When we consider only the shear strain, E_{me} and R can be rewritten as:

$$E_{me} = 2\mu\xi_{ij}^2 + 2B\xi_{ij}m_i m_j, \quad R = 2\eta\dot{\xi}_{ij}^2, \quad (34)$$

where $\mu = c_{44}$, and $\eta = \zeta_{44}$. In NSMMs, the direction of the crystal axis differs between the nanocrystallites, so it is impossible to describe the shear strain in the entire region using Eq. (34). However, since the total energy due to magnetostriction and the dissipation function are averaged within the exchange length, we can consider using isotropic elastic materials to clarify domain wall motion, and the shear strain can be described by Eq. (34). When the force acting on the displacement vector is balanced, we can obtain:

$$\dot{\xi}_{ij} + \lambda\xi_{ij} + \frac{B}{2\eta}m_i m_j = 0, \quad (35)$$

where λ is μ/η . Hence, the strain can be described by the integral of the magnetization:

$$\xi_{ij} = -\frac{B}{2\eta} \int_{-\infty}^t dt' m_i(t') m_j(t') e^{-\lambda(t-t')}. \quad (36)$$

This equation shows that the strain provides historical information on the magnetization when magnetic materials are viscous. In other words, the strain is delayed from the magnetic domain wall. The effective field due to magnetostriction can be obtained using the strain ξ_{ij} . The effective field can be calculated by the partial derivative of the total energy due to magnetostriction:

$$H_i^{me} = -\frac{1}{\mu_0 M_s} \frac{\partial E_{me}}{\partial m_i} = -\frac{2B}{\mu_0 M_s} \xi_{ij} m_j, \quad (37)$$

where M_s is the saturation magnetization and μ_0 is the vacuum permeability. Substituting Eq. (36), we can

obtain:

$$H_i^{\text{me}} = \frac{B^2}{\mu_0 M_s \eta} \int_{-\infty}^t dt' F_i(t, t') e^{-\lambda(t-t')}, \quad (38)$$

where:

$$F_i(t, t') = m_i(t') m_j(t') m_j(t). \quad (39)$$

The integral of Eq. (36) can be expanded by using integration by parts. After expanding the integration to the second order with respect to λ^{-1} , we can obtain:

$$\int_{-\infty}^t dt' F_i(t, t') e^{-\lambda(t-t')} = \frac{1}{\lambda} m_i(t) - \frac{1}{\lambda^2} \dot{m}_i(t) + O(\lambda^{-3}). \quad (40)$$

In this paper, we assumed that the terms above the third order can be neglected to simplify the problem. In this case, the torque T_{me} acting on the magnetization due to magnetostriction can be given as:

$$T_{\text{me}} = \lambda_s^2 D \mathbf{m} \times \frac{d\mathbf{m}}{dt}, \quad (41)$$

where:

$$D = \frac{9\gamma M_s}{\mu_0 M_s^2} \eta, \quad \lambda_s = -\frac{1}{3} \frac{B}{\mu}. \quad (42)$$

Hence, the effective field due to magnetostriction attenuates the rotation of the magnetization. The Landau–Lifshitz–Gilbert equation, including the effect of magnetostriction, can be written as:

$$\frac{d\mathbf{m}}{dt} = -\gamma \mathbf{m} \times \mathbf{H}^{\text{eff}} + (\alpha + \lambda_s^2 D) \mathbf{m} \times \frac{d\mathbf{m}}{dt}, \quad (43)$$

where α is the Gilbert damping constant and \mathbf{H}^{eff} is the effective field constructed by the exchange field and the external magnetic field.

When the frequency of the external magnetic field is low, soft magnetic materials are magnetized by the magnetic domain wall motion. The equation of magnetic domain wall motion can be directly obtained from the Landau–Lifshitz–Gilbert equation⁴³. Considering a 180° domain wall, the equation of motion is:

$$m\ddot{q} + \beta_{\text{dw}}\dot{q} + kq = 2\mu_0 M_s H_{\text{ext}}, \quad (44)$$

where q is the center position of the magnetic domain wall, m is the mass of the magnetic domain wall, k is the spring constant, H_{ext} is the external magnetic field, and

the damping coefficient β_{dw} can be written as:

$$\beta_{\text{dw}} = \frac{2\mu_0 M_s (\alpha + \lambda_s^2 D)}{\gamma \delta_w}, \quad (45)$$

where δ_w is the domain wall width. From Eq. (44), a time variation of the energy of the magnetic domain wall can be written as:

$$\frac{d}{dt} \left[\frac{m}{2} \dot{q}^2 + \frac{k}{2} q^2 \right] + \beta_{\text{dw}} \dot{q}^2 = W_{\text{dw}}, \quad (46)$$

where $W_{\text{dw}} = 2\mu_0 M_s H_{\text{ext}} \dot{q}$. This equation shows that the energy dissipation of the magnetic domain wall P_{dw} is:

$$P_{\text{dw}} = S \beta_{\text{dw}} \dot{q}^2 = S \beta_{\text{dw}} \kappa_{\text{dw}}^2 \dot{M}^2, \quad (47)$$

where S is the area of the magnetic domain wall, M is the magnetization of the entire soft magnetic material along the direction of the external magnetic field and κ_{dw} is a constant that converts the moving distance of the magnetic domain wall into the variation in the magnetization, as follows:

$$\Delta q = \kappa_{\text{dw}} \Delta M. \quad (48)$$

The magnetization process in soft magnetic materials is caused by the movement of numerous magnetic domain walls. In this case, the magnetization change caused by a single magnetic domain wall is $\Delta M/n_{\text{dw}}$, where n_{dw} is the number of magnetic domain walls, and the energy dissipation is:

$$P_{\text{dw}} = \frac{S \beta_{\text{dw}} \kappa_{\text{dw}}^2}{n_{\text{dw}}} \dot{M}^2. \quad (49)$$

G. Bertotti explained the frequency dependence of the anomalous eddy current loss by using local eddy currents due to domain wall motion^{16,44}. We formulated the energy loss associated with wall motion by considering magnetostriction instead of eddy currents. Analogous to W_{dw} , the energy dissipation due to the damping terms can be rewritten as:

$$P_{\text{dw}} = 2S\mu_0 M_s H_{\text{exc}} |\dot{q}|, \quad (50)$$

where:

$$H_{\text{exc}} = \frac{\beta_{\text{dw}} \kappa_{\text{dw}}}{2\mu_0 M_s n_{\text{dw}}} |\dot{M}|. \quad (51)$$

As the external magnetic field intensifies, the number of active domain walls n_{dw} increases because the pinned magnetic domain wall begins to move. As indicated by Eq. (46), the external magnetic field is partially consumed to increase the kinetic and potential energies of the magnetic

domain wall. To increase the number of active domain walls, the remaining magnetic field, i.e., H_{exc} , is used in magnetic domain wall depinning. Hence, in a simple approximation, the number of active domain walls can be written as:

$$n_{\text{dw}} = n_0 + \frac{H_{\text{exc}}}{V_0}, \quad (52)$$

where n_0 is the number of active domain walls in the absence of an external magnetic field and V_0 is the phenomenological parameter of the soft magnetic material. Substituting Eq. (52) into Eq. (51), H_{exc} can be rewritten as:

$$H_{\text{exc}} = \frac{n_0 V_0}{2} \left[\sqrt{1 + \frac{2\beta_{\text{dw}}\kappa_{\text{dw}}}{\mu_0 M_s n_0^2 V_0} |\dot{M}|} - 1 \right]. \quad (53)$$

When we consider the limit of high time variation in the magnetization, this magnetic field becomes:

$$H_{\text{exc}} = \sqrt{\frac{\beta_{\text{dw}} V_0 \kappa_{\text{dw}}}{2\mu_0 M_s} |\dot{M}|^{\frac{1}{2}}}. \quad (54)$$

Substituting Eq. (54) into Eq. (50), we can obtain:

$$P_{\text{dw}} = \sqrt{\beta_{\text{dw}} V_{\text{dw}} S \kappa_{\text{dw}}^3} |\dot{M}|^{\frac{3}{2}}, \quad (55)$$

where $V_{\text{dw}} = 2S\mu_0 M_s V_0$. The energy losses obtained in the experiments are time-averaged values caused by the numerous magnetic domain walls. Thus, the time variation in the magnetization can be roughly approximated as:

$$|\dot{M}| \sim M_{\text{max}} \frac{4}{T} = 4M_{\text{max}}f, \quad (56)$$

where M_{max} is the peak magnetization and T and f are the period and frequency, respectively, of the external magnetic field. Finally, the energy loss due to magnetostriction can be expressed as:

$$P_{\text{dw}} \sim 8\sqrt{\beta_{\text{dw}} V_{\text{dw}} S \kappa_{\text{dw}}^3} (M_{\text{max}}f)^{\frac{3}{2}}. \quad (57)$$

Note that Eq. (57) must be divided by the system volume to obtain the energy loss density. The energy loss due to magnetostriction has the same form as that of the anomalous eddy current loss. In the formulation in this paper, we considered the energy dissipation caused by magnetic domain wall motion inside a soft magnetic material with magnetostriction and viscosity. The energy dissipation mechanism does not depend on eddy currents. Hence, even when there is no eddy current present due to high resistance, the energy loss, which has the same frequency dependence as the anomalous eddy current loss, is caused by magnetostriction.

Results and discussion

The damping constant for the magnetic domain wall due to magnetostriction can be obtained by expanding the shear strain to the second order with respect to λ^{-1} , and the obtained damping constant is $\lambda_s^2 D$. The dimensionless parameter D is proportional to the viscosity constant. When the viscosity constant decreases to zero in Eq. (36), the strain is proportional to $m_i(t)m_j(t)$, and the torque due to magnetostriction vanishes. Hence, the dynamic viscosity is essential for the energy loss due to magnetostriction.

The viscosity constant can be obtained by dynamic viscoelastic measurements in which alternating stresses are applied to viscoelastic bodies. P. Rösner performed dynamic viscoelastic measurements of amorphous alloys to obtain a loss modulus G'' ⁴⁵. The loss modulus represents the energy dissipation of the viscoelastic body due to the viscosity, and we can obtain the viscosity constant using $\eta = G''/\omega$, where ω is the angular frequency of the alternating stress⁴⁶. According to Rösner's experiment, the viscosity constant is approximately 1.49×10^2 Pa·s at 350 K. Since a residual amorphous phase is contained in NSMMs, we used this value of the viscosity constant to analyze the energy loss due to magnetostriction.

Figure 5 shows the energy loss versus the frequency calculated by Eq. (57) for different magnetostriction constants. In the energy loss calculation, the saturation magnetization $\mu_0 M_s$ is 2.15 T, the vacuum permittivity μ_0 is 1.26×10^{-6} H/m, and the gyromagnetic ratio in the Landau–Lifshitz–Gilbert equation γ is 2.21×10^5 m/As, with $\alpha = 0.02$ and $\beta'_{\text{dw}} = 2\mu_0 M_s / \gamma \delta_w$. From these parameters, D becomes 1.38×10^8 . The frequency dependence of the energy loss due to magnetostriction is consistent with that of the excess losses observed in the experiments⁵, in which the electrical resistance of the magnetic material is high and the classical eddy current loss is suppressed. Thus, it is expected that the governing origin of the excess loss is magnetostriction. When the magnetostriction constant increases, the line of the energy loss shifts upward because the damping constant due to magnetostriction cannot be neglected compared to the Gilbert damping constant.

In the discussion of coercivity, magnetostriction is neglected in amorphous and NSMM alloys because its effects are limited. In contrast, magnetostriction significantly contributes to the energy loss caused by magnetic domain wall motion. Figure 6 shows the relationship between the energy loss due to magnetic domain wall motion and the magnetostriction constant λ_s . When the magnetostriction constant is close to zero, energy loss occurs due to the Gilbert damping constant^{47–49}. The energy loss increases linearly and attains almost the same value at the different Gilbert damping constants when the magnetostriction constant is greater than approximately

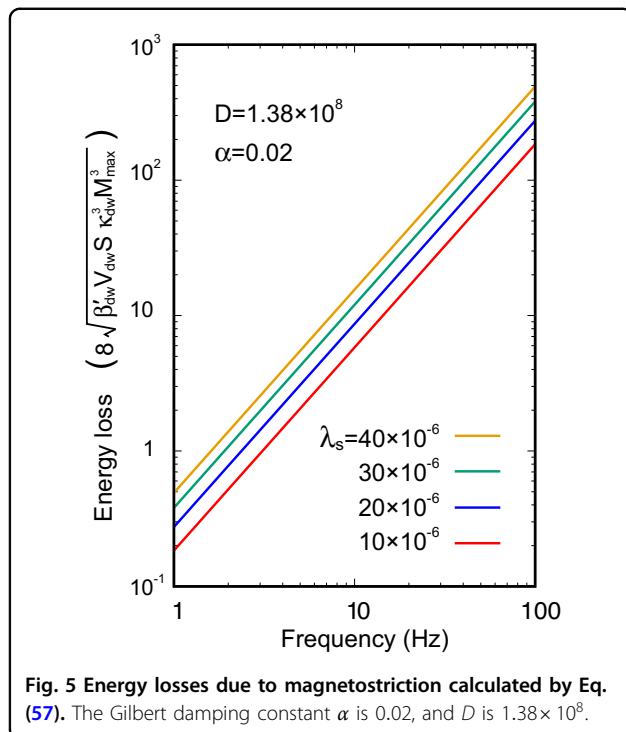


Fig. 5 Energy losses due to magnetostriction calculated by Eq. (57). The Gilbert damping constant α is 0.02, and D is 1.38×10^8 .

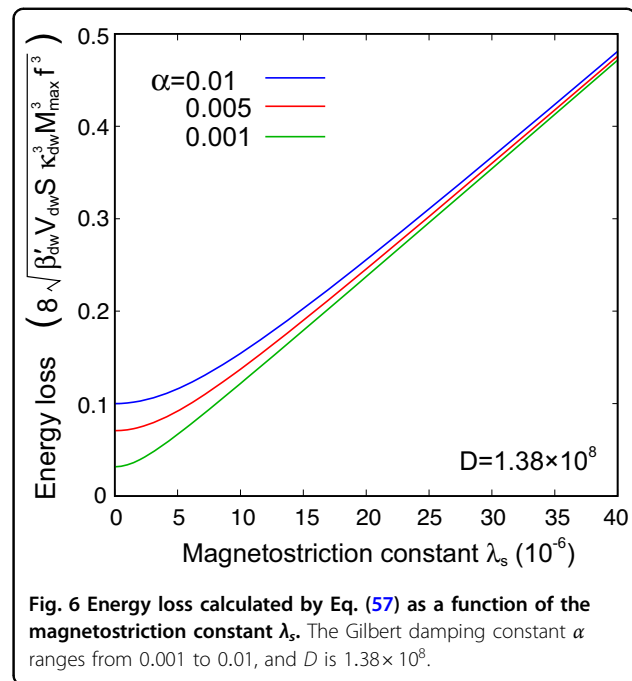


Fig. 6 Energy loss calculated by Eq. (57) as a function of the magnetostriction constant λ_s . The Gilbert damping constant α ranges from 0.001 to 0.01, and D is 1.38×10^8 .

20 ppm, i.e., the effect of magnetostriction dominates the energy loss.

To confirm the effect of magnetostriction on the dynamic loss behavior of soft magnetic materials, we performed core loss measurements of a commercial amorphous alloy (Fe₈₀Si₉B₁₁) and a range of nanocrystalline (nc) alloys. Magnetic hysteresis curves under an alternating current (AC) field were measured on an Iwatsu SY-8219 B-H analyzer at 2 kHz. Static hysteresis curves were also acquired on a DC B-H tracer. The details of the DC and AC hysteresis measurements, including the sample geometry and coil configurations, are available elsewhere. Four disc-shaped samples with a diameter of 10 mm were used with strain gauges for measuring the saturation magnetostriction. The saturation magnetostriction λ_s of the alloys are $40 \pm 2 \times 10^{-6}$ for the amorphous alloy, $25.6 \pm 2 \times 10^{-6}$ for nc-(Fe_{0.8}Co_{0.2})₈₆B₁₄, $14 \pm 2 \times 10^{-6}$ for nc-Fe₈₆B₁₃Cu₁, $2.4 \pm 0.5 \times 10^{-6}$ for nc-Fe₈₀Nb₆B₁₄ and near zero ($\sim 10^{-7}$) for nc-Fe₈₅Nb₆B₉.

Figure 7 shows the AC hysteresis curves acquired at 2 kHz for these 5 alloys. The maximum magnetic polarization was limited to 1 T for all the measurements. In each AC hysteresis plot, a static minor loop obtained by the DC B-H tracer with the same maximum polarization is also shown for comparison. This is denoted by the hysteresis loss in the plots. We also estimated the classical eddy current loss at 2 kHz by following Bertotti's approach, where the additional field due to the eddy current was predicted using Maxwell's equations⁴⁴. The

results are included in the AC hysteresis loops. Hence, the residual area of each AC hysteresis loop after subtracting both the static hysteresis loss and the classical eddy current loss corresponds to the excess loss component, often referred to as the anomalous eddy current loss.

Regardless of the samples investigated here, the classical eddy current loss is only a minor component of the total loss at 2 kHz because of the small sample thickness of the melt-spun ribbons (typically between 15 and 25 μm). In contrast, the excess loss component varies considerably depending on the saturation magnetostriction. The excess loss component remains a minor component for the near zero-magnetostrictive nc-Fe₈₅Nb₆B₉, and the core loss at 2 kHz is governed primarily by the hysteresis loss, whereas the excess loss governs the total loss for the amorphous alloy with a large λ_s value.

Figure 8 shows the change in the excess loss (i.e., the area of the excess loss in Fig. 7 multiplied by the frequency) as a function of λ_s . Notably, the excess loss linearly increases with saturation magnetostriction, revealing that the energy dissipation due to magnetostriction dominates the excess loss, and the excess loss attains a finite value even when the magnetostriction constant approaches zero. Since these behaviors are fully consistent with those of the analytical calculation results shown in Fig. 6, the experimental results verify the formulation of the magnetostrictive effect on the energy loss.

The effect of magnetostriction on the coercivity caused by residual strains has been examined in terms of its slight effect. The results of this paper indicated that

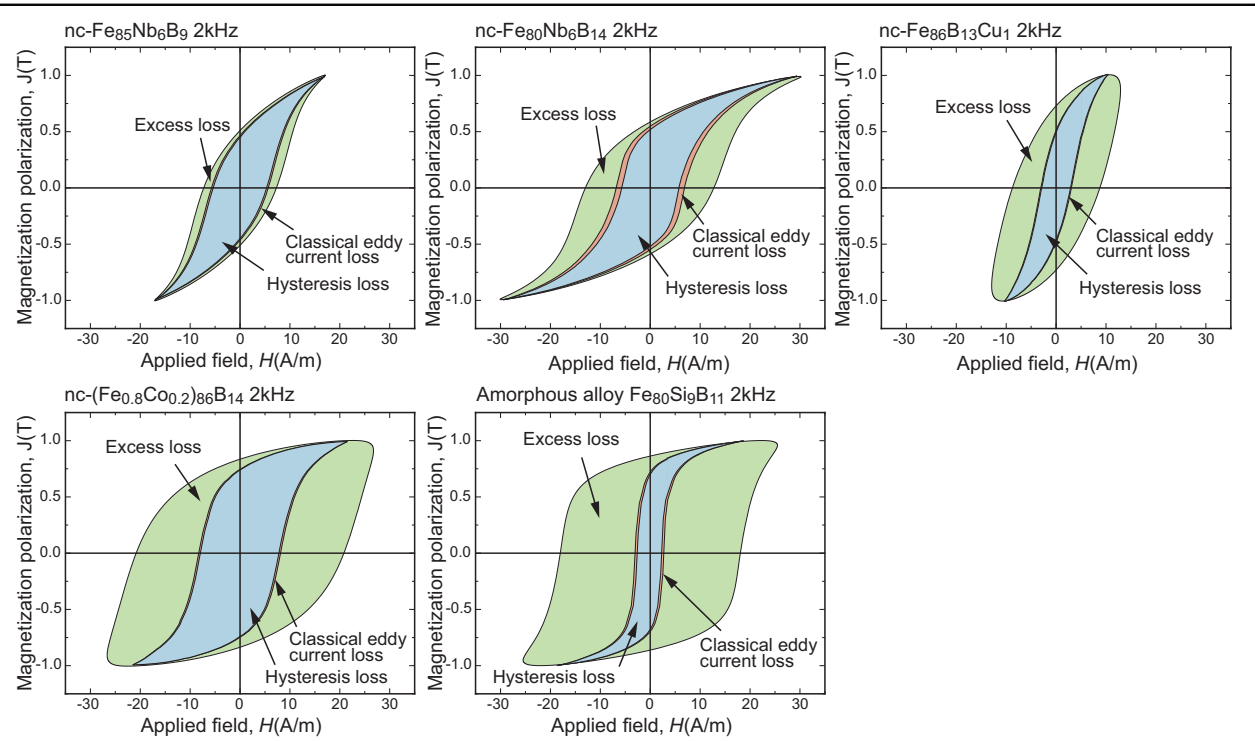


Fig. 7 AC hysteresis curves of nanocrystalline and amorphous alloys observed in the experiments. Cyan and orange indicate the contributions of the hysteresis loss and classical eddy current loss, respectively. Green denotes the excess loss, i.e., the remaining energy loss.

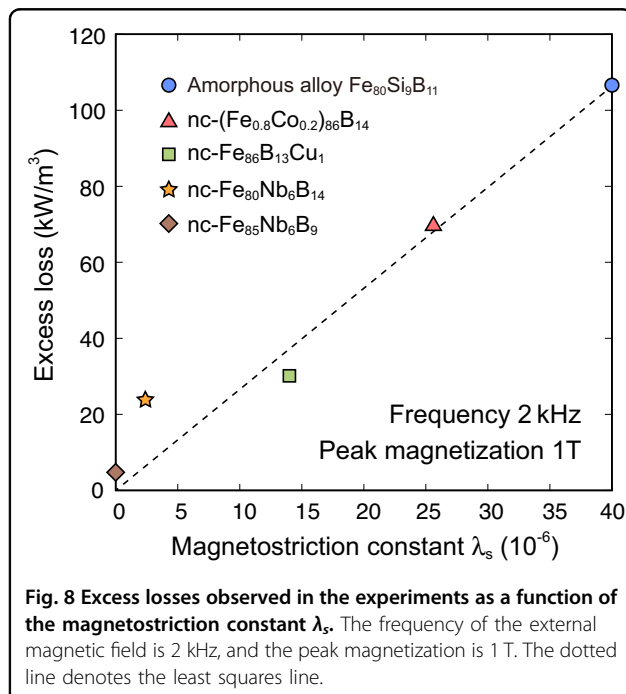


Fig. 8 Excess losses observed in the experiments as a function of the magnetostriction constant λ_s . The frequency of the external magnetic field is 2 kHz, and the peak magnetization is 1 T. The dotted line denotes the least squares line.

magnetostriction directly contributes to the energy loss due to the viscosity of the magnetic material. The energy loss in soft magnetic materials can be explained by the

sum of the hysteresis loss, classical eddy current loss, and anomalous eddy current loss, but magnetostriction also generates energy loss with the same frequency dependence as the anomalous eddy current loss. Thus, the total energy loss of the soft magnetic material P_{total} can be decomposed as:

$$P_{\text{total}} = P_{\text{hys}} + P_{\text{ec}} + P_{\text{ex}}, \quad (58)$$

where P_{hys} is the hysteresis loss, P_{ec} is the classical eddy current loss and P_{ex} is the excess loss. Both the anomalous eddy current loss P_{ea} and P_{dw} are components of P_{ex} , and if their contributions can be summed linearly, P_{ex} can be expressed as:

$$P_{\text{ex}} = P_{\text{ea}} + P_{\text{dw}}. \quad (59)$$

These two components are indistinguishable from each other in terms of frequency dependence. However, for amorphous and NSMMs, the energy loss due to magnetostriction dominates the excess loss. Consequently, the focus of alloy development in these classes of materials should be to reduce the saturation magnetostriction.

Conclusion

The analytical calculations clarified how magnetostriction causes energy loss in NSMMs, and this mechanism

was validated by experiments. In NSMMs, homogeneous and heterogeneous strains are caused by distortions of each nanocrystallite due to magnetostriction. Since the magnetoelastic energy caused by heterogeneous strains is reduced by averaging within the exchange length, the effect of magnetostriction on the magnetic anisotropy is decreased. In contrast, the magnetic anisotropy due to the homogeneous strain is not averaged by the randomness of the crystal axes of the nanocrystallites and yields the same effect as the induced magnetic anisotropy. However, this magnetic anisotropy due to magnetostriction cannot explain the excess loss observed in the experiments because the effect on the magnetic anisotropy is limited.

If a magnetic domain wall is present, the magnetic material is distorted by magnetostriction to stabilize the total energy of the magnetic domain wall. As the magnetic domain wall moves, the local strain also changes to reduce the total energy. However, the change in the strain is retarded with respect to magnetic domain wall motion due to the viscosity of the magnetic material. This retardation could generate a viscous resistance acting on the magnetic domain wall.

Following H. Suhl, we formulated the viscous resistance of the magnetic domain wall motion due to magnetostriction by considering only the shear strain. The viscous resistance increases with the square of the magnetostriction constant and is proportional to the viscosity constant. The energy loss due to magnetic domain wall motion can be obtained by using this viscous resistance, according to G. Bertotti. The obtained energy loss exhibits the same frequency dependence as the anomalous eddy current loss, and this dependence is consistent with the experimental observations. In the discussion of coercivity, the contribution of magnetostriction is negligible, but the energy loss due to magnetic domain wall motion is dominated by the energy dissipation caused by magnetostriction. The clarification of the new energy loss mechanism due to magnetostriction provides useful suggestions for improving the energy efficiency of soft magnetic materials.

Acknowledgements

This work was supported by the MEXT Program—Data Creation and Utilization-Type Material Research and Development Project (Digital Transformation Initiative Center for Magnetic Materials), Grant Number JPMXP1122715503, and Toyota Motor Corporation. K.O. was partly supported by the JST-Mirai Program, Grant Number JPMJMI19G1. The authors would like to express their sincere thanks to H. Imamura and A. Kato for their useful discussions.

Author details

¹Department of Applied Physics, Osaka University, Osaka 565-0871, Japan.

²Institute of Multidisciplinary Research for Advanced Materials, Tohoku University, Sendai 980-8577, Japan. ³Department of Materials Science and Engineering, Monash University, Clayton, VIC 3800, Australia

Author contributions

The authors confirm the following contributions to this paper: research conception and design: H.T. and K.S.; formulation of theory and calculation:

H.T.; measurements and data analysis: H.H. and K.S.; draft manuscript preparation: H.T. and K.S. This study was performed under the supervision of K.S. and K.O. All authors reviewed the results and approved the final version of the manuscript.

Conflict of interest

The authors declare no competing interests.

Publisher's note

Springer Nature remains neutral with regard to jurisdictional claims in published maps and institutional affiliations.

Received: 31 August 2023 Revised: 16 January 2024 Accepted: 13 February 2024

Published online: 26 March 2024

References

- McCoy, G. A., Litman, T., & Douglass, J. G. *Energy-Efficient Electric Motor Selection Handbook* (Bonneville Power Administration, 1990).
- Herzer, G. Modern soft magnets: amorphous and nanocrystalline materials. *Acta Mater.* **61**, 718–734 (2013).
- Silveyra, J. M., Ferrara, E., Huber, D. L. & Monson, T. C. Soft magnetic materials for a sustainable and electrified world. *Science* **362**, eaao0195 (2018).
- Parsons, R. et al. Core loss of ultra-rapidly annealed Fe-rich nanocrystalline soft magnetic alloys. *J. Magn. Magn. Mater.* **476**, 142–148 (2019).
- Huang, H. et al. Effect of grain size on the core loss of nanocrystalline $Fe_{68}B_{13}Cu_1$ prepared by ultra-rapid annealing. *AIP Adv.* **13**, 025304 (2023).
- Alben, R., Becker, J. J. & Chi, M. C. Random anisotropy in amorphous ferromagnets. *J. Appl. Phys.* **49**, 1653–1658 (1978).
- Herzer, G. Grain size dependence of coercivity and permeability in nanocrystalline ferromagnets. *IEEE Trans. Magn.* **26**, 1397–1402 (1990).
- Herzer, G. Soft magnetic nanocrystalline materials. *Scr. Metall. Mater.* **33**, 1741–1756 (1995).
- Suzuki, K. & Cadogan, J. M. Random magnetocrystalline anisotropy in two-phase nanocrystalline system. *Phys. Rev. B* **58**, 2730–2739 (1998).
- Willard, M. A., Francavilla, T. & Harris, V. G. Core-loss analysis of an (Fe, Co, Ni)-based nanocrystalline soft magnetic alloy. *J. Appl. Phys.* **97**, 10F502 (2005).
- Graham, C. D. Physical origin of losses in conducting ferromagnetic materials (invited). *J. Appl. Phys.* **53**, 8276–8280 (1982).
- Williams, H. J., Shockley, W. & Kittel, C. Studies of propagation velocity of a Ferromagnetic domain boundary. *Phys. Rev.* **80**, 1090–1094 (1950).
- Fish, G. E. Soft magnetic materials. *Proc. IEEE* **78**, 947–972 (1990).
- Sakaki, Y. An approach estimating the number of domain walls and eddy current losses in grain-oriented 3% Si-Fe tape wound cores. *IEEE Trans. Magn.* **16**, 569–572 (1980).
- Sakaki, Y. & Imagı, S. Relationship among eddy current loss, frequency, maximum flux density and a new parameter concerning the number of domain walls in polycrystalline and amorphous soft magnetic materials. *IEEE Trans. Magn.* **17**, 1478–1480 (1981).
- Bertotti, G. General properties of power losses in soft ferromagnetic materials. *IEEE Trans. Magn.* **24**, 621–630 (1988).
- Inomata, K., Hasegawa, M., Kobayashi, T. & Sawa, T. Magnetostriction and magnetic core loss at high frequency in amorphous Fe-Nb-Si-B alloys. *J. Appl. Phys.* **54**, 6553–6557 (1983).
- Suzuki, K., Makino, A., Inoue, A. & Matsumoto, T. Low core losses of nanocrystalline Fe-M-B (M=Zr, Hf, or Nb) alloys. *J. Appl. Phys.* **74**, 3316–3322 (1993).
- Tsukahara, H., Imamura, H., Mitsumata, C., Suzuki, K. & Ono, K. Role of magnetostriction on power losses in nanocrystalline soft magnets. *NPG Asia Mater.* **14**, 44 (2022).
- Lee, E. W. Magnetostriction and magnetomechanical effects. *Rep. Prog. Phys.* **18**, 189–229 (1955).
- Wang, H. et al. Ab initio studies of the effect of nanoclusters on magnetostriction of $Fe_{1-x}Ga_x$ alloys. *Appl. Phys. Lett.* **97**, 262505 (2010).
- Zhang, Y., Wang, H. & Wu, R. First-principles determination of the rhombohedral magnetostriction of $Fe_{100-x}Al_x$ and $Fe_{100-x}Ga_x$ alloys. *Phys. Rev. B* **86**, 224410 (2012).

23. Wang, H., Zhang, Z. D., Wu, R. Q. & Sun, L. Z. Large-scale first-principles determination of anisotropic mechanical properties of magnetostrictive Fe–Ga alloys. *Acta Mater.* **61**, 2919 (2013).

24. Wang, H. et al. Understanding strong magnetostriction in $Fe_{100-x}Ga_x$ alloys. *Sci. Rep.* **3**, 3521 (2013).

25. Jones, N. J. et al. Rhombohedral magnetostriction in dilute iron (Co) alloys. *J. Appl. Phys.* **117**, 17A913 (2015).

26. Wang, H. & Wu, R. First-principles investigation of the effect of substitution and surface adsorption on the magnetostrictive performance of Fe–Ga alloys. *Phys. Rev. B* **99**, 205125 (2019).

27. Yang, Z. et al. Large magnetostriction of heavy-metal-element doped Fe-based alloys. *J. Appl. Phys.* **132**, 215105 (2022).

28. Sander, D. The correlation between mechanical stress and magnetic anisotropy in ultrathin films. *Rep. Prog. Phys.* **62**, 809–858 (1999).

29. Yoshizawa, Y., Oguma, S. & Yamauchi, K. New Fe-based soft magnetic alloys composed of ultrafine grain structure. *J. Appl. Phys.* **64**, 6044–6046 (1988).

30. Suzuki, K., Kataoka, N., Inoue, A., Makino, A. & Matsumoto, T. High saturation magnetization and soft magnetic properties of bcc Fe–Zr–B alloys with ultrafine grain structure. *Mater. Trans. JIM* **31**, 743–746 (1990).

31. Hono, K., Hiraga, K., Wang, Q., Inoue, A. & Sakurai, T. The microstructure evolution of a $Fe_{73.5}Si_{13.5}B_9Nb_3Cu_1$ nanocrystalline soft magnetic material. *Acta Met. mater.* **40**, 2137–2147 (1992).

32. Makino, A., Hatanai, T., Inoue, A. & Matsumoto, T. Nanocrystalline soft magnetic Fe–M–B (M = Zr, Hf, Nb) alloys and their applications. *Mater. Sci. Eng. A* **226–228**, 594–602 (1997).

33. Zhang, J. X. & Chen, L. Q. Phase-field microelasticity theory and micromagnetic simulations of domain structures in giant magnetostrictive materials. *Acta Mater.* **53**, 2845–2855 (2005).

34. Khachaturyan, A. G. *Theory of Structural Transformations in Solid*, (Wiley, New York, NY, 1983).

35. Herzer, G. The random anisotropy model. *Properties and Applications of Nanocrystalline Alloys from Amorphous Precursors*. NATO Science Series, Vol. 184, 17. (Springer, Dordrecht, 2005).

36. Suzuki, K., Herzer, G. & Cadogen, J. M. The effect of coherent uniaxial anisotropy on the grain-size dependence of coercivity in nanocrystalline soft magnetic alloys. *J. Magn. Magn. Mater.* **177–181**, 949–950 (1998).

37. Schäfer, R., Hubert, A. & Herzer, G. Domain observation on nanocrystalline material. *J. Appl. Phys.* **69**, 5325–5327 (1991).

38. Rührig, M. et al. Domain observations on Fe–Cr–Fe layered structures. Evidence for a Biquadratic Coupling Effect. *Phys. Stat. Sol. (a)* **125**, 635–656 (1991).

39. Flohrer, S. et al. Dynamic magnetization process of nanocrystalline tape wound cores with transverse field-induced anisotropy. *Acta Mater.* **54**, 4693–4698 (2006).

40. Pieper, W. & Gerster, J. Total power loss density in a soft magnetic 49% Co–49% Fe–2% V-alloy. *J. Appl. Phys.* **109**, 07A312 (2011).

41. Landau, L. D. and Lifshitz, E. M. *Theory of Elasticity*, 3rd edn, p. 100 (Pergamon, New York, 1986).

42. Suhl, H. Theory of the magnetic damping constant. *IEEE Trans. Magn.* **34**, 1834–1838 (1998).

43. Malozemoff, A. P. & Slonczewski, J. C. *Magnetic Domain Walls in Bubble Materials* (Academic Press, New York, 1979).

44. Bertotti, G. *Hysteresis in Magnetism* (Academic Press, San Diego, CA, 1998).

45. Rösner, P., Samwer, K. & Lunkenheimer, P. Indications for an “excess wing” in metallic glasses from the mechanical loss modulus in $Zr_{65}Al_{7.5}Cu_{27.5}$. *Europhys. Lett.* **68**, 226–232 (2004).

46. Tropea, C. and Yarin, A. L. *Springer Handbook of Experimental Fluid Mechanics* (Springer Science & Business Media, 2007).

47. Beatrice, C., Bottauscio, O., Chimapi, M., Fiorillo, F. & Manzin, A. Magnetic loss analysis in Mn–Zn ferrite cores. *J. Magn. Magn. Mater.* **304**, e743–e745 (2006).

48. Beatrice, C. et al. Magnetic loss, permeability dispersion, and role of eddy currents in Mn–Zn sintered ferrites. *J. Magn. Magn. Mater.* **320**, e865–e868 (2008).

49. Fiorillo, F., Coisson, M., Beatrice, C. & Pasquale, M. Permeability and losses in ferrites from dc to the microwave regime. *J. Appl. Phys.* **105**, 07A517 (2009).